Self-Trapping of Optical Beams through Thermophoresis

Yuval Lamhot, Assaf Barak, Or Peleg, and Mordechai Segev
Physics Department, Technion, Haifa 32000, Israel
(Received 15 July 2010; published 15 October 2010)

We demonstrate, theoretically and experimentally, self-trapping of optical beams in nanoparticle suspensions by virtue of thermophoresis. We use light to control the local concentration of nanoparticles, and increase their density at the center of the optical beam, thereby increasing the effective refractive index in the beam vicinity, causing the beam to self-trap.

DOI: 10.1103/PhysRevLett.105.163906 PACS numbers: 42.65.Tg, 42.65.Jx, 42.65.Wi

Self-channeling of optical beams in fluidic suspensions—liquids containing small particles—has been studied since 1982 [1,2], when it was demonstrated that the optical gradient force can give rise to self-trapped beams. For almost three decades, theoretical papers studying the general concept of self-channeling in fluids have been numerous [2], but experiments have been scarce [1]. The effects leading to self-channeling of light in fluid suspensions can be classified in two general classes: effects relying on light scattering, i.e., the optical gradient force [1], and thermal effects relying on (weak) absorption, either in the fluid or in the particles [3]. When the particles are much smaller than the optical wavelength, the gradient force is very weak; hence, one would need a high density to cause a significant change in the refractive index to trap narrow beams. However, at higher particle densities, multiple scattering becomes dominant, randomizing the direction of scattered light. This works against the tendency of the gradient force to push the particles (with refractive index higher than of the liquid) towards the beam center. In addition, particle-particle interactions further limit this optically induced concentration process [4]. Consequently, it is difficult to self-trap very narrow beams through the gradient force because this requires high particle densities, which in turn involves multiple scattering, which acts as effective loss. Thermal effects, on the other hand, can lead to a significant refractive index change, but in pure liquids the refractive index typically decreases with increasing temperature, which can support dark solitons [3] but not self-trapping of (bright) beams. Hence, an additional mechanism is required for self-trapping of optical beams in thermal fluids.

Here, we demonstrate, theoretically and experimentally, self-trapping of optical beams in nanoparticle suspensions by virtue of thermophoresis. Our experiments manifest a new kind of interplay between light, nanoparticles, and liquids. This ability to use light to control the local concentration of nanoparticles in a liquid has major implications for a variety of applications, such as using light to locally control chemical reactions, diffusion, osmosis, catalysis, etc.

Thermophoresis, a thermal mechanism often observed in colloidal suspensions, manifests a strong reaction of the suspended particles to temperature gradients. Thermophoresis, or the Sôret effect, describes the ability of a macromolecule or particles to drift along a temperature gradient [5,6]. In a thermal gradient, a colloidal particle attains a drift velocity $v_T = -D_T \nabla T$, where D_T is the thermophoretic mobility. The direction of the thermal drift is determined by the sign of D_T, making the particles concentrate in hotter regions or in colder regions of the fluid (positive or negative thermophoresis, respectively). At temporal steady state, thermophoretic transport is balanced by Brownian diffusion, as the Sôret coefficient, $S_T = D_T/D$, constituting the ratio between D_T and the Brownian diffusion coefficient. In the absence of thermal convection, Sôret coupling of heat and mass transfer leads to a steady-state concentration depending solely on the temperature distribution within the fluid. Considerable effort has been made in recent years to understand the fundamentals of thermophoretic motion [5,6]. For negative thermophoresis, the particles are thermophillic, moving from colder regions to hotter ones. Negative thermophoresis typically occurs for a polar solvent, where charges at the surface of the particles give rise to ordering of the molecules around them or to changing of the hydration entropies at the particle-solution interface [5]. Qualitative temperature dependence of S_T suggests that the thermodiffusion of charged particles in aqueous solutions is highly dependent on the response of water molecules to the high electric field of the double layer [6]. Namely, negative thermophoresis appears when the particle size decreases to nanometric scales, and it depends on the solvent properties (temperature, pH, concentration of particles, etc.). Many nanoparticle suspensions and macromolecules exhibit a negative Sôret coefficient: nanometric polystyrene spheres, silica nanospheres, organic macromolecules, proteins, various DNA or RNA strains, and more.

When the refractive indices of the particles and the liquid are different, thermophoresis can be utilized to change the local optical properties of a solution by redistributing the particles suspended in it. We show that a beam propagating in such a fluid can give rise to a refractive index profile that guides the beam, thereby generating a ''hot-particle soliton'' [7]. To do this, one should use a proper combination of particles and liquid with a negative

Sôret coefficient. The beam should be slightly absorbed in the fluid and act as a heat source. The negative thermophoresis gives rise to particles concentrating at the region where the temperature is elevated, i.e., the center of the beam. If the particles have a refractive index higher than that of the liquid ($n_{\text{particle}} > n_{\text{solution}}$), under negative thermophoresis they increase the refractive index at the beam center, thereby creating a waveguide [8]. When the structure of the beam inducing this waveguide coincides with the wave function of the guided mode within the waveguide, the beam self-traps, forming a spatial soliton. Such a thermophoresis-based soliton has never been suggested or observed. This ability to redistribute nanoparticles with light at the precision of tens of micrometers is attractive for many applications, especially because producing a meaningful gradient force on nanometric particles requires very high optical intensities [1]. This mechanism can serve as a means to concentrate nanoparticles with light and arrange them at prescribed structures within the liquid. Such nonlinear optofluidic interaction could be utilized to control chemical and biological reactions, to separate between particles of different sizes or compositions, to arrange molecules, etc.

We model this system in temporal steady state, where the temperature distribution T in the fluid is described by the heat equation with a ''source'' term: the optical intensity I absorbed within the fluid with an absorption coefficient α,

$$-k_{\text{th}}\nabla_{\perp}^2 T = \alpha I(1), \tag{1}$$

where k_{th} is the heat conductance in the fluid. If the absorption is due to the liquid only, the coefficient is multiplied by $(1 - V_f)$, where V_f is the local volume fraction of the particles. Strictly speaking, when the absorption is also included in the optical wave equation, there are no solitons—because a source that decays with propagation inevitably leads to nonstationary solutions. However, in our experiments, absorption is so small that the light is practically nondepleted for propagation distances L of tens of cm. Hence we neglect absorption in the wave equation.

In order to model the temperature dependence of the local volume fraction of the particles, we use the empirical expression for the single-particle Sôret coefficient [5],

$$S_T(T) = S_{T,\infty}\left[1 - \exp\left(\frac{T^* - T}{T_0}\right)\right], \tag{2}$$

where $S_{T,\infty}$ is the high temperature limit, T^* the temperature at which the sign of S_T changes, and T_0 represents the strength of the temperature effect. Here, $S_T < 0$ for $T < T^*$. The function rises relatively fast and appears to reach a constant value at high temperature. Utilizing S_T, we can calculate the distribution of the particles in the solution, in temporal steady state, to be

$$\vec{\nabla}_{\perp} C = -C S_T \vec{\nabla}_{\perp} T, \tag{3}$$

where C describes the nanoparticle concentration. For the simplest soliton, we seek propagation-invariant solutions; i.e., Eq. (3) contains derivatives in x, y only. For small volume fractions of particles ($V_f < 3\%$), the Sôret coefficient is independent of the concentration [6]; hence, Eq. (3) leads to the following relation for local volume fraction,

$$V_f(\vec{r}) = V_{f,0}\exp\left(-\int_{T_0}^{T(\vec{r})} S_T dT\right), \tag{4}$$

where $V_{f,0}$ is such that it keeps the average volume fraction constant (total amount of nanoparticle does not change). From Eq. (4) we see that for $S_T < 0$ the local V_f increases in areas where the temperature is higher, thereby raising the refractive index in that region (recall $n_{\text{particle}} > n_{\text{solution}}$). The refractive index for a nanoparticle suspension with $V_f \ll 1$ can be approximated as $n_0 \cong n_{\text{particle}} V_f + n_{\text{solution}}(1 - V_f)$. In our experiments, we can neglect the thermal dependence of n_{particle}; hence, the local change in the refractive index can be approximated by

$$\frac{\partial n}{\partial T} = (n_{\text{particle}} - n_{\text{solution}})\frac{\partial V_f}{\partial T} + \left(\frac{\partial n_{\text{solution}}}{\partial T}\right)(1 - V_f). \tag{5}$$

For most fluids $\partial n_{\text{solution}}/\partial T < 0$; therefore, in pure liquids raising the temperature will cause the refractive index to decrease and a thermal defocusing effect will occur. For a colloidal dispersion with $n_{\text{particle}} > n_{\text{solution}}$ and $\partial V_f/\partial T > 0$, the overall thermal change in the refractive index can be made positive, thereby creating a focusing effect for the beam whose absorption is what induces the process. For this to occur, the particles must be thermophilic. The spatial distribution of the refractive index change is computed by calculating the index as a function of local temperature T and particle concentration C, and subtracting the initial index n_o,

$$\Delta n = n(T, V_f(T)) - n_0(T_0, V_{f,0}), \tag{6}$$

Equations (1)–(5) are supplemented by the nonlinear paraxial wave equation for a monochromatic field $E_{\text{opt}}(x, y, z, t) = A(x, y, z)\exp[i(kz - \omega t)]$ of a slowly varying envelope $A(x, y, z)$ [9],

$$i\frac{\partial A}{\partial z} + \frac{1}{2k}\nabla_{\perp}^2 A + \frac{k\Delta n}{n_0}A = 0, \tag{7}$$

where z is propagation direction, $k = 2\pi n_0/\lambda_0$ is the wave number in the medium (λ_0 is the vacuum wavelength). The intensity profile is $I = |A|^2$.

The simplest solitons correspond to solutions with z invariant T, C, Δn, with $A(x, y, z) = U(x, y)\exp[-i\gamma z]$. We solve the equations in a self-consistent manner: we place an initial guess for I in Eq. (1), from which we find the temperature profile $T(x, y)$, which we substitute in Eq. (2) and find $S_T(x, y)$. With $S_T(x, y)$ we use Eq. (4) to find the local volume fraction of particles, which we use in Eq. (6) to find Δn. Substituting Δn in Eq. (7), we calculate the modified A caused by the new refractive index. We place this $I = |A|^2$ back in Eq. (1) to calculate $T(x, y)$ again, and from it the rest of the variables. We iterate until the profiles converge. These propagation-invariant solutions yield the

properties of the soliton for a given parameter set (average volume fraction, total beam power, etc.).

In finding solitons, we use the experimental parameters of our system, along with some values from handbooks. We use aqueous dispersion of thermophilic 20 nm diameter polystyrene (PS) particles (water suspension of PS nanosphere standard by Duke Thermo Scientific), whose S_T was studied extensively [5], from which the values of $S_{T,\infty}$, T^*, and T_0 were taken. In our suspension, $S_T < 0$ for $T < 45\,^{\circ}\mathrm{C}$; hence, room temperature is adequate for thermophillic transport. Our initial average volume fraction is $V_{f,0} = 1\%$. We use a fluid cell with a square cross section of 1 mm^2. The wavelength of the beam is $\lambda = 808$ nm, at which the refractive index of the nanoparticles is higher than that of water ($n_{\mathrm{aq}} = 1.29$, $n_{\mathrm{PS}} = 1.69$). The absorption in our suspension is mostly in the water due to O-H bonds, with $\alpha = 2\ \mathrm{m}^{-1}$. The propagation length in our cell is $L \sim 1$ cm, giving $\alpha L \ll 1$. The thermal boundary conditions at the cell walls can be set either to a constant temperature or to be insulating. These conditions determine the ambient temperature of the fluid, which controls the thermal behavior of the particles because S_T is temperature dependent. Our calculations account for the actual dimensions of the cell including the thickness of the walls, which affect $T(x, y)$ in Eq. (1). The model neglects convective flow in the fluid, because buoyancy currents are negligible, as the Rayleigh number is much smaller than the critical value.

Using the self-consistency method described above, we explore the properties of the hot-particle soliton. Figure 1 displays the results for an ambient temperature of 20 °C for two opposing cell walls, while the other two walls are thermally insulating. Figures 1(a)–1(d) show the FWHM of the hot-particle soliton, maximal index change $\Delta n_{\max}$, maximal temperature change, and maximal concentration, as a function of the beam power. The soliton FWHM decreases as the power is increased. Importantly, from $\Delta n_{\max}$ we see that the hot-particle solitons are stable according to the Vakhitov-Kolokolov criterion. As expected, $\Delta n_{\max}$ increases as the power is increased. Notice the large change in the particles' concentration at the beam center—in excess of 1.5—manifesting a very large effect. Solutions with other initial concentrations indicate that—as $V_{f,0}$ is smaller—this accumulation factor increases (the factor is 2.5 for $V_{f,0} = 0.5\%$, 3.5 for $V_{f,0} = 0.3\%$). Figures 1(e)–1(g) show the various profiles for ΔT, accumulation factor, and beam intensity, for a soliton beam with a power of 600 mW and 30 μm FWHM. The cross section of each plot is shown by the white line at the bottom of 1(e)–1(g). Notice that the particles' concentration resembles the profile of the ΔT, which happens as long as $S_T \Delta T \ll 1$. Such concentration profile gives rise to the induced waveguide, whose guided mode is the beam profile of Fig. 1(g).

Having found the stationary (soliton) solution, we now simulate the propagation dynamics by solving the above

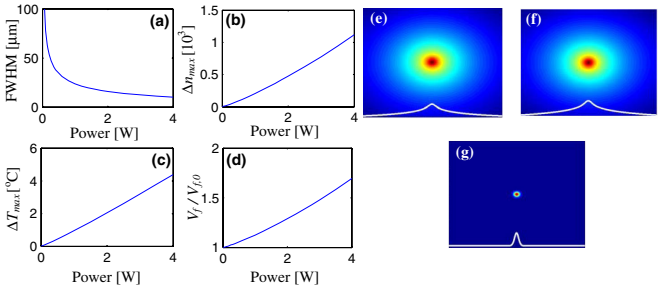

FIG. 1 (color online). Properties of the hot-particle soliton as a function of beam power. (a) FWHM, (b) $\Delta n_{\max}$, (c) $\Delta T_{\max}$, and (d) relative maximal concentration, and the profiles of (e) ΔT, (f) particle concentration, and (g) the beam intensity for a 0.6 W soliton beam.

equations numerically, under various initial conditions. Figure 2(a) shows the propagation dynamics of the 30 μm FWHM beam of Fig. 1(g), at 0.6 W power ($P_{30\ \mu\mathrm{m}} = 0.6$ W) under the thermal boundary conditions described above, with and without thermophoresis. Here, $L = 1$ cm ($\alpha L = 0.02$). As shown in Fig. 2(a), in the thermophoretic medium the beam maintains a constant width throughout propagation, whereas without thermophoresis the beam FWHM increases to $\sim$70 μm. Figure 2(b) shows the propagation dynamics of a beam with the same wave function (the 30 μm FWHM stationary solution) but at different beam powers. For power smaller than $P_{30\ \mu\mathrm{m}}$, the beam broadens with z (the smaller the power, the greater the broadening). For power higher than $P_{30\ \mu\mathrm{m}}$, the beam first undergoes overfocusing, and then begins oscillatory evolution, as typical to self-focusing media when the input beam is somewhat broader than the soliton solution.

We perform experiments with the above parameters in a 1 cm long fluid cell of a 1 mm^2 square cross section, placed between two thermoelectric coolers which set the temperature at the outer surface of two opposing faces of the cell. The fluid is the 20 nm polystyrene spheres dispersed in water with $V_{f,0} = 1\%$. We launch a 30 μm FWHM Gaussian beam and image the output beam.

Figure 3 displays the experimental results as a function of beam power. Our system yields a stable soliton at $\sim$1 W power, for which the output beam has the same width as the

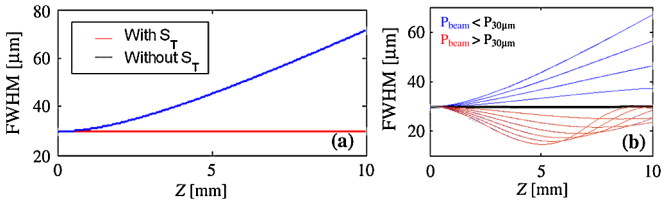

FIG. 2 (color online). (a) Propagation dynamics for a $P_{30\ \mu\mathrm{m}} = 0.6$ W soliton beam in the thermophoretic media and in plain water. (b) Dynamics for the same 30 μm FWHM beam, for powers above (red) and below (blue) $P_{30\ \mu\mathrm{m}}$ (supporting stationary propagation of a soliton, bold black line).

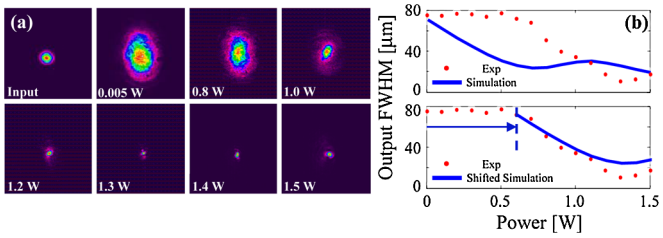

FIG. 3 (color online). Experimental results. (a) Intensity profiles for a 30 μm FWHM input beam: input beam and output beams for varying input power. (b) Measured FWHM of the output beam as a function of the input power, compared to the calculated results, with and without the 0.6 W shift signifying the unexpected threshold effect.

30 μm FWHM input beam. Experimentally, we observe a noticeable self-focusing effect for beam power >0.5 W. This effect, which continuously narrows the beam, continues for higher powers, until at 1.3 W the output beam begins to broaden again, corresponding to an oscillatory propagation dynamics—as expected when self-focusing is too strong for the input beam to form a soliton. The focusing effect occurs within a few seconds. We measure the width of the focused output beam for several hours and no major change is seen. In all cases, there are small fluctuations in both the location and the shape of the beam, but the value of the FWHM varies by only $\pm 2.5\%$. The effect is fully reversible: for a high power focused beam, once the power is lowered below 0.5 W the FWHM of the output beam returns to its original broad state within seconds.

Figure 3(b), showing the width of the output beam as a function of input beam power, displays a threshold effect, which was not predicted by the model. Clearly, for beam power below 0.6 W, no change is observed in the output beam width. Namely, a significant waveguiding effect appears only above this threshold value of beam power. Comparing the experiments and the calculated results reveals that the figures are shifted by ~ 0.6 W. Apart from this shift, the figures coincide. This shift between the experiments and the calculated results is also observed with other parameters, e.g., varying the temperature (from 10 °C to 25 °C), and lowering the initial volume fraction ($V_{f,0} = 0.35, 0.5\%$). In all cases, the theoretical figure is shifted with respect to the experiments by ~ 0.6 W. This shift between our model and the experimental results might be explained in several ways. As stated above, no noticeable change in the output beam is observed for low-power input beams for several hours. On the other hand, when the beam power is higher than the threshold value, the change in output beam width is fast (several seconds). Therefore, the origin of the threshold is not the dynamic behavior of the system, neither is it the lack of time needed for the effect to be fully developed. The threshold effects might originate from the values of the Sôret coefficient used in the model. The empiric expression for the Sôret effect states that S_T is a constant, whereas in reality it is possible that the coefficient depends on the gradient or on the thermophoretic motion, which could have a threshold temperature gradient for the particles to begin their motion. Altogether, apart from the shift in the soliton existence curve, the model explains the results very well.

To summarize, we predicted and observed a new type of self-trapped beams: hot-particle soliton, forming in nanoparticles suspension by virtue of thermophoresis. These experiments manifest a new kind of interplay between light and fluid. This ability to use light to control the local concentration of nanoparticles in a liquid has major implications for a variety of applications, ranging from using light to locally control chemical reactions, diffusion, osmosis, and catalysis, to symbiotic nonlinear dynamics of light and fluids.

This work was supported by an Advanced Grant from the European Research Council and by the Israel Science Foundation.

[1] A. Ashkin, J. M. Dziedzic, and P. W. Smith, Opt. Lett. **7**, 276 (1982); V. E. Yashin *et al.*, Opt. Spectrosc. **98**, 466 (2005); P. J. Reece, E. M. Wright, and K. Dholakia, Phys. Rev. Lett. **98**, 203902 (2007); M. Anyfantakis *et al.*, Opt. Lett. **33**, 2839 (2008); W. M. Lee *et al.*, Opt. Express **17**, 10277 (2009).

[2] C. Conti, G. Ruocco, and S. Trillo, Phys. Rev. Lett. **95**, 183902 (2005); R. El-Ganainy *et al.*, Opt. Express **15**, 10207 (2007); Opt. Lett. **32**, 3185 (2007); R. Gordon, J. T. Blakely, and D. Stinton, Phys. Rev. A **75**, 055801 (2007); M. Matuszewski, W. Krolikowski, and Y. S. Kivshar, Opt. Express **16**, 1371 (2008).

[3] G. A. Swartzlander *et al.*, Phys. Rev. Lett. **66**, 1583 (1991); B. Luther-Davies and Y. Xiaoping, Opt. Lett. **17**, 496 (1992).

[4] R. El-Ganainy *et al.*, Phys. Rev. A **80**, 053805 (2009).

[5] S. Duhr and D. Braun, Phys. Rev. Lett. **96**, 168301 (2006); Proc. Natl. Acad. Sci. U.S.A. **103**, 19 678 (2006); S. Iacopini, R. Rusconi, and R. Piazza, Eur. Phys. J. E **19**, 59 (2006); R. Piazza and A. Parola, J. Phys. Condens. Matter **20**, 153102 (2008); M. Braibanti, D. Vigolo, and R. Piazza, Phys. Rev. Lett. **100**, 108303 (2008).

[6] S. A. Putnam and D. G. Cahill, Langmuir **21**, 5317 (2005); **23**, 9221 (2007); H. Ning *et al.*, Langmuir **24**, 2426 (2008); N. Ghofraniha, C. Conti, and G. Ruocco, Phys. Rev. B **75**, 224203 (2007); N. Ghofraniha *et al.*, Phys. Rev. Lett. **102**, 038303 (2009); N. Ghofraniha, G. Ruocco, and C. Conti, Langmuir **25**, 12 495 (2009); Y. Lamhot *et al.*, Phys. Rev. Lett. **103**, 264503 (2009).

[7] We use the term "spatial soliton" to describe a self-trapped beam, not necessarily in an integrable system. For a review on optical solitons, see G. I. Stegeman and M. Segev, Science **286**, 1518 (1999).

[8] The particle accumulation also overcompensates for the thermal decrease of the refractive index in the liquid.

[9] R. W. Boyd, *Nonlinear Optics* (Academic, New York, 2003).